The Relation Among Porosity, Permeability, and Specific Surface of Chalk From the Gorm Field, Danish North Sea

ARTICLE *in* SPE RESERVOIR EVALUATION & ENGINEERING · JUNE 1998

Impact Factor: 0.99 · DOI: 10.2118/31062-PA

3 AUTHORS, INCLUDING:

Ida L. Fabricius
Technical University of Denmark
121 PUBLICATIONS **969** CITATIONS

The Relation Among Porosity, Permeability, and Specific Surface of Chalk From the Gorm Field, Danish North Sea

Jeanette Mortensen,* SPE, Technical U. of Denmark, **Finn Engstrøm,** SPE, Mærsk Oil and Gas A/S, and **Ida Lind,** SPE, Technical U. of Denmark

Summary

The origin of the difference in the relationship between permeability and porosity for Danian and Maastrichtian chalk from the Gorm field offshore Denmark has been investigated. The investigation was based on 300 sets of core data (He-expansion porosity and air permeability) from Well Gorm N-22X. On 24 of the core plugs, the specific surface was determined by BET and, on 14 of these samples, image analysis was made.

The data were rationalized by the use of the Kozeny equation and it was found that each geologic unit had a characteristic relationship among porosity, permeability, and specific surface. Furthermore, it was found that the nature of porosity (intrafossil, intergranular, etc.) had no significant influence on the air permeability, so that the permeability of the chalk can be calculated from total porosity and specific surface.

Kozeny's empirical constant, c, was determined analytically from a simple porosity model and Poiseuille's law.

Introduction

Experience has illustrated that to a first approximation, porosity and the logarithm of permeability are well correlated in the North Sea chalk.[1] However, different stratigraphical units have distinctly different porosity-permeability relations. For a given porosity, the permeability of chalk of Maastrichtian age is, e.g., on average, larger than the permeability of chalk of Danian age. The cause for the differences in porosity-permeability relationships between the chalk units is not well documented in literature, but the size of pores and particles, and the surface characteristics of the particles are likely controlling factors.

This study was undertaken to obtain a simple model for the relationship among porosity, permeability, and specific surface for reservoir chalk irrespective of stratigraphic unit, and to evaluate the usefulness of image-analysis data relative to laboratory data. To meet this purpose, we have studied core data from a chalk field (the Gorm field) applying the Kozeny equation.[2]

Preliminary Data Review

The Gorm field is producing from Danian and Maastrichtian chalk located in the Danish North Sea (**Fig. 1**).[3,4] An earlier investigation of the Gorm chalk indicates that the matrix permeability for this material is practically isotropic on a cm scale.[5] Variations in the porosity-permeability correlation for Gorm chalk can, therefore, be assumed to be solely a function of the basic rock properties, because the effect of directional anisotropy can be ignored. A preliminary screening of core data illustrated that the investigated chalk sequence could be divided into three separate depth/age intervals with different porosity-permeability relationships (**Fig. 2**). The three intervals are of the Danian, late Maastrichtian, and early Maastrichtian Ages. The Danian chalk is characterized by a relatively high amount of larger grains and intrafossil porosity, whereas the Maastrichtian chalk has more uniform grain size and only little intrafossil porosity (**Fig. 3**). The Maastrichtian grains also appear smoother than the Danian. These observed textural differences indicate that the differences in porosity-permeability correlations for Danian and Maastrichtian chalk could be attributed to differences in grain size and surface area. The effect of grain size on permeability is commonly studied by image analysis, and the effect is attributed to pore morphology.[6] In the present study, we assume that the grain-pore interfacial resistance is the dominant force as predicted by Kozeny.[2]

Theory and Previous Work

Kozeny's equation originates from soil mechanics and forms the basis for one of several approaches to understanding permeability.[7] This approach was chosen for the present study for its simplicity. It is based on Kozeny's derivation of a theoretical relationship for laminar flow of a fluid in a porous medium.[2] The equation states that the permeability can be related to the physical properties of a rock as follows.

$$k = c\frac{\phi^3}{s^2} = c\frac{\phi^3}{(1-\phi)^2 \cdot s_s^2} = c\frac{\phi^3 \cdot d^2}{(1-\phi)^2 \cdot 6^2}, \quad \ldots\ldots\ldots\ldots (1)$$

where k is the liquid permeability, ϕ is porosity, S is grain-surface area per bulk volume, S_s is specific surface (grain-surface area per grain volume), and d is equivalent spherical diameter. The value of d is determined by combining the equations for the grain-surface area $A = \pi \cdot d^2$ and the grain volume $V = \frac{1}{6} \cdot \pi d^3$ into the expression $S_s = A/V = 6/d$. The factor c is Kozeny's constant. According to Poiseuille's law, c will have a value of 0.5 for parallel circular tubes. On the basis of experimental data on porous material, Kozeny found that c for natural materials has a value of 0.22 to 0.24.

Carman[8] applied Kozeny's equation and replaced the constant, c, by the expression,

$$c = \frac{1}{k_o \cdot (L_a/L)^2}, \quad \ldots\ldots\ldots\ldots\ldots\ldots\ldots\ldots\ldots\ldots (2)$$

where k_o is a dimensionless shape factor, L_a is the actual flow length through the porous medium, and L is the sample length. $(L_a/L)^2$ is commonly referred to as the tortuosity. Carman[8] concluded that k_o is near 2 for laminar flow-through channels, irrespective of cross sections being circular or noncircular. For the tortuosity, from observation of the flow path of dyed liquid, he believed 2 was a reasonable value for packed spheres. Carman's value for c (0.25) is, therefore, close to Kozeny's value for c (0.22 to 0.24).

The work of Kozeny and Carman was applied to petroleum reservoirs by Wyllie,[9] and several other authors have obtained empirical relationships among grain size, grain sorting, and permeability of sand and sandstones[10-12] in general accordance with the pattern obtained by Kozeny. Panda and Lake[13] derived an expression for permeability based on parameters of particle-size distribution by assuming a tortuosity of 3. This relationship, however, is only valid for permeabilities above 1 Darcy and, thus, not applicable to chalk.

*Now with Mærsk Oil and Gas A/S.

Original SPE manuscript received for review 4 August 1995. Revised manuscript received 4 February 1998. Paper (SPE 31062) peer approved 20 February 1998.
*Now with with Mærsk Oil and Gas A/S.

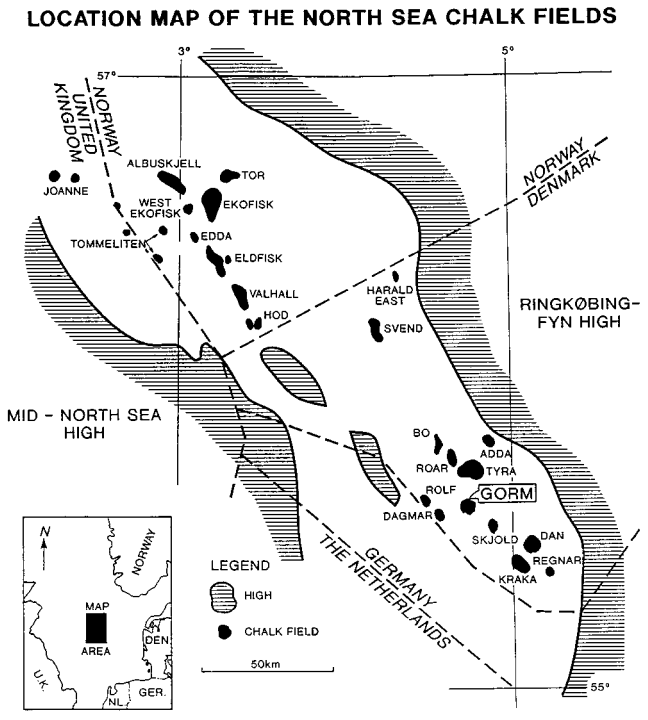

Fig. 1—Location of the Gorm field. (Modified after Ref. 4).

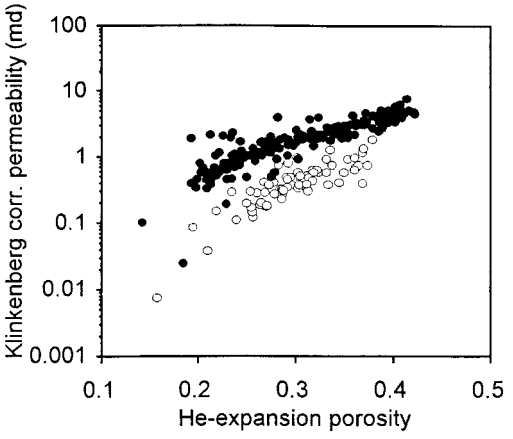

Fig. 2—Klinkenberg-corrected air permeability data vs. He-expansion-porosity data for core plugs of Well N-22X. Black dots are Maastrichtian samples. White dots are Danian samples.

Theory and Present Study

For the present study of chalk with isotropic low permeability, we applied the work of Kozeny directly to avoid the ambiguities related to tortuosity. We modeled the chalk as a system of orthogonal interpenetrating tubes (see Appendix) and assumed that the tubes only conduct the fluid in a direction parallel to the flow. This means that a part of the porosity is ineffective. The proportion of ineffective porosity is a function of the porosity, as expressed in a porosity-dependent Kozeny factor, c. For porosities ranging from 20 to 40%, we obtain c factors from 0.21 to 0.24, in agreement with the observations of Kozeny.[2]

Fig. 4 demonstrates our application of Kozeny's equation. Here, the calculated permeability is shown as a function of porosity for constant values of the equivalent spherical-grain diameter. Note that the equivalent spherical diameter is a direct measure of specific surface without any presumptions about grain shape. The function approaches zero permeability for zero porosity and unbounded permeability for 100% porosity, as expected. A logarithmic scale is chosen for the permeability, in accordance with conventional porosity-permeability crossplots.

Data and Measurements

The applicability of Kozeny's equation to chalk was tested by analysis of core data from a 100-m cored interval in Well N-22X in the Gorm field. He-expansion-porosity and air-permeability data were available from about 300 plugs from this well. All permeability measurements had been done under conditions of laminar flow. Before further analysis, measured air-permeability data, K_a, measured at a pressure drop of 7 to 15 psi, were converted to Klinkenberg permeability, K_k, by means of the following correlation developed by Mærsk Oil and Gas A/S (**Fig. 5**).

$$K_k = 0.52 \cdot K_a^{1.083}. \quad \ldots\ldots\ldots\ldots\ldots\ldots\ldots\ldots\ldots\ldots (3)$$

He-expansion-porosity and air-permeability data for the entire dataset were reviewed, and a subset of 24 plugs, covering the entire range of porosity-permeability and chalk units, was selected for further analysis. The purpose of the further analysis was to determine the physical properties of the chalk samples, which were expected to influence the porosity-permeability relation according to the Kozeny equation (i.e., the nature of the porosity, grain size distribution, and specific surface). Determination of the specific surface by BET (N_2 adsorption) was done for the entire subset. For BET, plug slices of approximately 1 g, divided into approximately 40 pieces, were used. A grain density of 2.71 g/cm^3 was used for recalculating the specific surface from m^2/g to 1/μm.

Image analysis of backscatter electron micrographs of polished plug-slice surfaces was done on 14 of the 24 samples. The analyses were performed by means of the Pippin® image-analysis program, based on the principles of Niblack.[14] Images with 300X magnification were used to measure intrafossil porosity and percentage of larger grains, whereas images with the maximal obtainable magnification of 3000X were used to measure matrix porosity, specific surface, and grain-size distribution of matrix grains. For detection of a possible influence on He-expansion-porosity data from porosity type, the total porosity was calculated from image-analysis data by combining intrafossil porosity, amount of larger grains, and matrix porosity. These total-porosity data were calibrated by a constant factor obtained by correlating image analysis and laboratory-porosity data for samples without intrafossil porosity. For the calculation of grain-size distribution, a Pippin de-agglomeration procedure was applied. Specific surface from image analysis was estimated by means of a purpose-built mathematical filter, which counts the pixels at the boundaries between porosity and solid phase, and which takes the orientation of the boundaries into account.

Results and Discussion

Table 1 lists the results from core analysis and image analysis of the selected subset of samples from Well N-22X. The data include the Klinkenberg corrected air permeability and the permeability calculated from He-expansion porosity and BET data, by means of the c values listed in **Table 2**. These c values are derived directly from the model presented in the Appendix, and are, thus, analytically determined. Between the logarithm of the calculated and the measured permeability, a correlation coefficient R^2 of 0.96 was obtained, demonstrating the validity of Kozeny's equation (**Fig. 6**). Although Danian samples have intrafossil porosity, this apparently has no influence on the accordance with Kozeny's equation. This indicates that all measured porosity is available for gas transport. If the intrafossil porosity had been closed in relation to air permeability, but not to porosity measurements, the porosity used in the calculations would have been too high, as would the calculated permeabilities.

That the intrafossil porosity is not closed to gas transport is supported by the observation that porosities determined by image analysis are similar to the laboratory measurements, as indicated by a R^2 of 0.89 (**Fig. 7**). The image-analysis porosity includes intrafossil porosity, and the linear relation indicates that the laboratory measurements also do so. In accordance with our results, Donaldsen *et al.*,[15] for glass spheres and crushed sand, found excellent agreement between measured permeability and permeability determined from BET and ϕ by means of Kozeny's equation and a c factor of 0.2. Interestingly, they found that the permeability

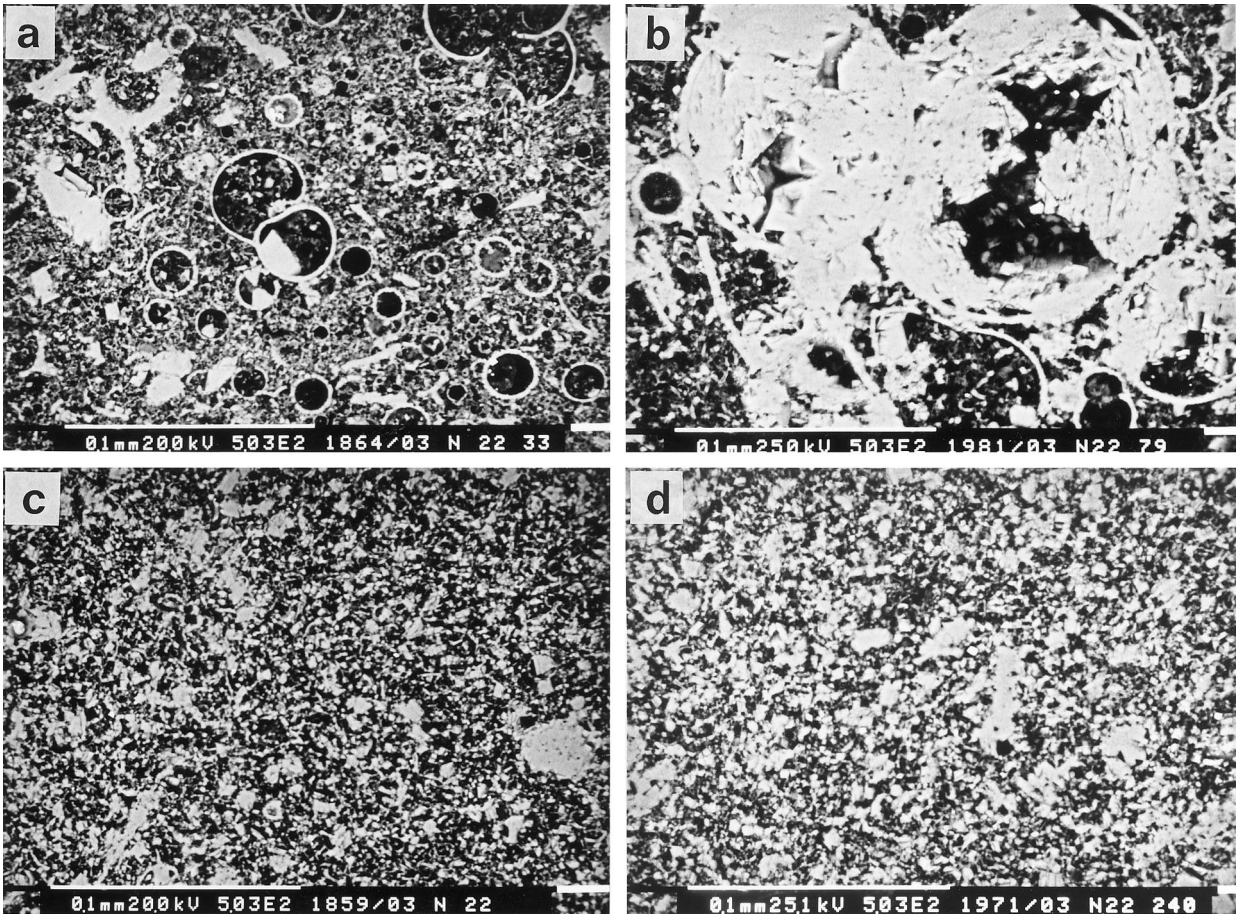

Fig. 3—BSE images of polished chalk samples from Well N-22X of the Gorm field. The white scale bars have a length of 0.1 mm. (a) Danian chalk characterized by the presence of intrapartcle porosity in addition to the intergranular porosity. Note the irregularity of the grains. The sample has a He-expansion porosity of 36%. Sample depth is 2099 m below mean sea level. (b) Sample from the lower 10 ft of the Danian interval. This interval is characterized by the high abundance of larger grains. The sample has an He-expansion porosity of 30%. Sample depth is 2114 m below mean sea level. (c) Maastrichtian chalk characterized by intergranular porosity and smoother grain surfaces. The sample has an He-expansion porosity of 36%. Sample depth is 2147 m below mean sea level. (d) Sample from the lower part of the cored Maastrichtian interval. Note relatively large uniform grain size. The sample has an He-expansion porosity of 29%. Sample depth is 2160 m below mean sea level.

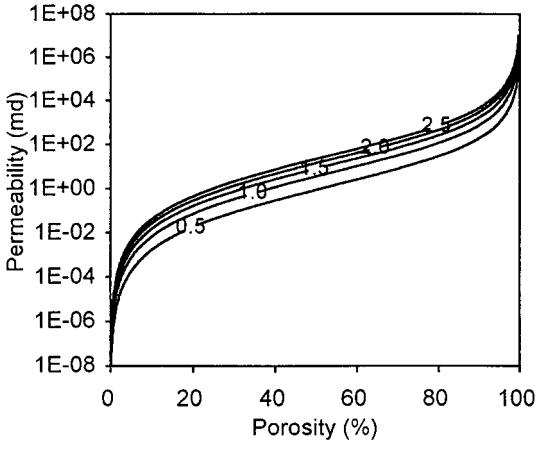

Fig. 4—The relationship between permeability and porosity as calculated from the equation of Kozeny[2] under the assumption of porosity-dependent *c*-factor (Appendix 1). Each curve represents one equivalent spherical grain diameter, indicated in μm.

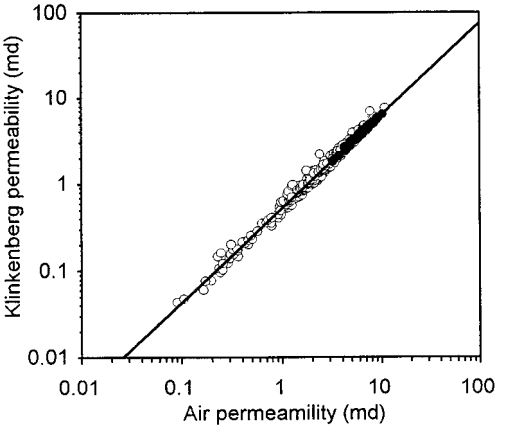

Fig. 5—Klinkenberg permeability vs. standard air permeability (800 psi), Black dots are Maastrichtian samples. White dots are Danian samples.

of natural sand was considerably larger than predicted from ϕ and BET. The reason for this is probably the crushed surface of natural sand. That a similar effect is not seen in chalk may be because the surfaces of even irregular chalk particles are smooth crystal planes.

Fig. 8 demonstrates the difficulty of obtaining the specific surface from image analysis. For the Maastrichtian samples, with relatively smooth grains and small specific surface, it is possible to predict the specific surface by image analysis of 3000X-magnified polished samples, whereas the method fails for the more irregular Danian samples, where the specific surface is high, and the

TABLE 1—CORE-ANALYSIS AND IMAGE-ANALYSIS DATA FOR SAMPLES FROM WELL N-22X.

Age	Measured Depth (ft)	He-Expansion Porosity (%)	Klinkenberg Corrected Permeability (md)	BET-Specific Surface Relative to Grains (m^2/g)	BET-Specific Surface Relative to Grains ($1/\mu m$)	Image Analysis data: Matrix Porosity (%)	Intrafossil Porosity (%)	Massive Grains (%)	Total Porosity (%)	Specific Surface ($1/\mu m$)	Average Diameter of Matrix Particles (μm)
Danian	6989.2	33.8	0.75	2.69	7.30						
Danian	7005.0	32.4	0.58	2.42	6.56	38	6.9	19	33.8	4.15	1.5
Danian	7021.0	36.1	0.98	2.44	6.60	35	9.0	11	36.0	4.54	1.4
Danian	7028.0	28.7	0.30	3.19	8.64	35	6.6	20	30.8	4.19	1.4
Danian	7031.0	26.4	0.19	2.98	8.08	43	4.1	21	35.3	4.38	1.3
Danian	7043.2	25.6	0.15	2.93	7.94						
Danian	7049.6	31.4	0.48	2.45	6.63						
Danian	7060.3	24.0	0.11	3.24	8.79						
Danian	7064.0	26.1	0.28	1.87	5.08	51	6.4	48	28.6	3.88	1.4
Danian	7068.3	30.2	0.98	1.53	4.14	57	2.8	42	32.9	3.91	1.3
Danian	7070.7	27.9	0.58	2.02	5.48	56	5.3	47	30.9	3.22	1.5
Maastrichtian	7075.6	35.9	4.21	0.97	2.63	36	1.4	7	33.8	2.90	2.3
Maastrichtian	7105.9	38.7	4.61	1.10	2.99						
Maastrichtian	7139.9	41.2	4.61	1.37	3.71	45	0.1	2	43.2	4.14	1.0
Maastrichtian	7159.7	38.7	3.55	1.41	3.82						
Maastrichtian	7178.7	36.2	3.29	1.20	3.25	39	0.2	3	36.3	3.13	2.2
Maastrichtian	7199.4	28.0	1.65	0.92	2.48	31	0.2	17	25.0	2.29	3.0
Maastrichtian	7220.3	30.1	1.65	0.95	2.58						
Maastrichtian	7243.7	19.9	0.46	0.77	2.10						
Maastrichtian	7269.1	27.5	1.34	1.04	2.83						
Maastrichtian	7291.3	29.3	1.83	0.93	2.51	33	0.2	10	29.2	2.92	2.5
Maastrichtian	7298.1	25.3	1.04	1.01	2.75	33	1.1	14	28.5	2.64	2.4
Maastrichtian	7304.1	21.0	0.52	0.97	2.63	26	0.8	11	23.3	2.34	2.7
Maastrichtian	7330.1	22.6	0.69	0.85	2.31						

TABLE 2—KOZENY'S FACTOR, *c*, AS CALCULATED FROM POROSITY, ϕ

ϕ (%)	*c* circular tubes	*c* square tubes
0	0.17	0.17
20	0.21	0.21
40	0.24	0.23
60	0.27	0.27
80	0.33	0.32
100	0.50	0.50

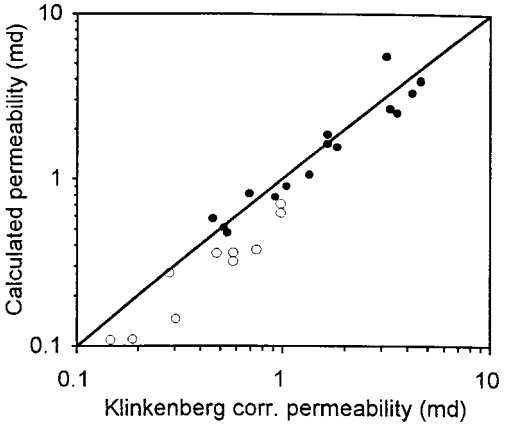

Fig. 6—The permeability calculated from the laboratory data for specific surface, porosity, and density vs. the Klinkenberg-corrected air permeability. Black dots are Maastrichtian samples. White dots are Danian samples.

pixels used for image analysis are large compared to the grain surface irregularities.

An equivalent spherical diameter of grains can be obtained from the BET measurements of specific surface. The equivalent spherical diameters determined from BET data correspond well to the ones predicted from Kozeny's equation (**Fig. 9**). This indicates that it is the specific surface, rather than the actual grain diameters, that determines the relationship between porosity and permeability.

The data on Fig. 9 fall in three groups. One group has equivalent spherical-grain diameter of approximately 1 μm and porosities ranging from 25 to 35%. This group represents Danian samples (Fig. 3a), and covers an interval of 25 m. Another group has equivalent spherical diameters of approximately 2 μm and porosities ranging from 30 to 45%. These samples are from the uppermost 40 m of the Maastrichtian interval (Fig. 3c). The third group is from the subsequent 30 m of the Maastrichtian (Fig. 3d). Equivalent spherical diameters in this group are near 2.5 μm and the porosity ranges from 20 to 30%. The first two groups are connected by a 3-m-thick transition zone with equivalent spherical diameters ranging from 1 to 2.5 μm and porosities between 25 and 35% (Fig. 3b). Each of them has a uniform specific surface. This

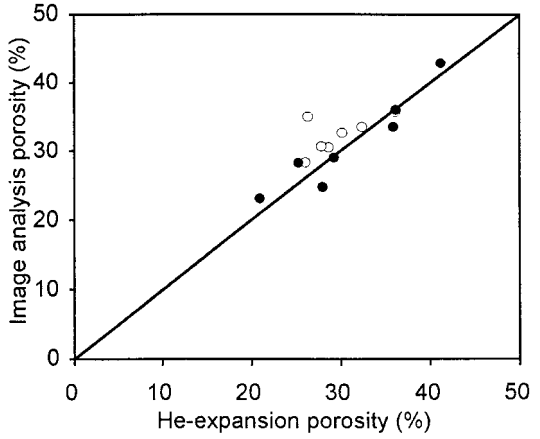

Fig. 7—The porosity determined by image analysis of electron micrographs of polished surfaces vs. the porosity measured in the laboratory. Black dots are Maastrichtian samples. White dots are Danian samples.

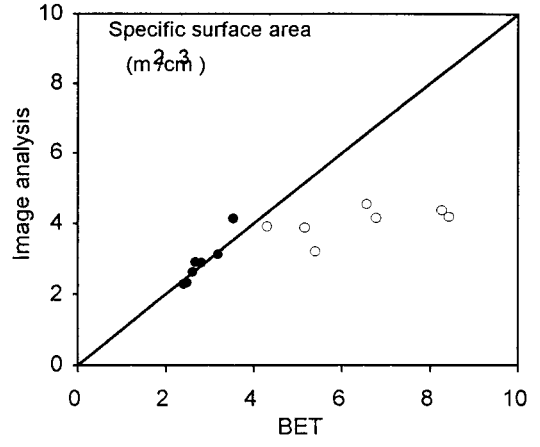

Fig. 8—The ratio between grain surface area and grain volume. Values determined by image analysis of electron micrographs of polished surfaces vs. values based on laboratory measurements of specific surface and density. Black dots are Maastrichtian samples. White dots are Danian samples.

means that the air-permeability and porosity data fall along a line of uniform, equivalent spherical diameter.

Conclusion

For the present chalk samples from the Gorm field, the following conclusions can be drawn.

1. Based on a simple porosity model, Kozeny's factor c has been analytically shown to vary from 0.21 to 0.24 for porosities of 20 to 40%.

2. The permeability of small chalk samples, k, can be calculated from porosity, ϕ, and the specific surface (relative to grain volume), S_s, by the formula,

$$k = c\frac{\phi^3}{(1-\phi)^2 \cdot s_s^2}. \quad \ldots\ldots\ldots\ldots\ldots\ldots\ldots\ldots\ldots\ldots (4)$$

3. Each lithologic unit has a characteristic specific surface (a constant ratio between grain-surface area and grain volume). This figure remains roughly constant over depth intervals of 20 to 40 m despite varying porosity, and it determines the relation between porosity and permeability.

4. The specific surface, rather than the grain size, determines the permeability. The main division of units corresponds to chalk intervals of Danian and Maastrichtian Age.

5. For the samples studied, the nature of the porosity has no influence on the air permeability. Permeabilities for samples with a significant amount of intrafossil porosity can be predicted equally well as permeabilities for samples with only interparticle porosity.

6. BSE images yield a porosity in general correspondence with the He-expansion porosity.

7. The determination of specific surface by image analysis fails for particles with large ratios between surface area and grain volume. The reason for this must be that the size of the image pixels are too large to resolve the irregularity of the surface of grains with high specific surface.

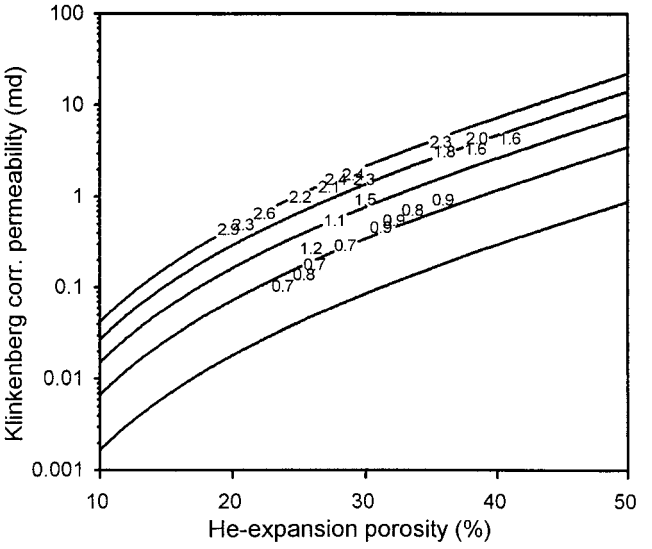

Fig. 9—Klinkenberg-corrected air permeability vs. the He-expansion porosity. Each data point is annotated by the equivalent spherical diameter (in μm) of the grains, as calculated from the specific surface. The curves of Fig. 4 are shown as a reference.

Nomenclature

c = Kozeny's factor
d = equivalent sphere diameter, L, μm
k = permeability, L^2, md
k_0 = shape factor (=2, for tubes)
$k_{\delta S_{wir}}$ = permeability for oil at irreducible water saturation, L^2, md
L = sample length, L, μm
L_a = flow length through porous medium, L, μm
r = radius, L, μm
r_h = hydraulic radius, L, μm
R^2 = correlation coefficient
S = surface area per bulk volume, 1/L, 1/μm
S_s = specific surface, surface area per grain volume, 1/L, 1/μm
V = volume
θ = angle, degrees
ϕ = porosity
ϕ_{af} = porosity, which is active for flow in a specific direction

Acknowledgments

The authors thank Mærsk Oil and Gas A/S and the Partners of the Dansk Undergrunds Consortium, A.P. Møller, Shell, and Texaco for permission to publish this paper. A. Aa. Nielsen, K. Carlsen, I. Søndergaard (DTU) and N. Springer (Geological Survey of Denmark) are thanked for advice and technical support.

References

1. Scholle, P.A.: "Chalk Diagenesis and Its Relation to Petroleum Exploration: Oil From Chalks, a Modern Miracle?" *AAPG Bull.* (1977) **61**, 982.
2. Kozeny, J.: "Über kapillare Leitung des Wassers im Boden," *Sitzungsberichte der Wiener Akademie der Wissenschaften* (1927) **136**, 271.
3. Hurst, C.: "Petroleum Geology of the Gorm Field, Danish North Sea," *Petroleum Geology of the Southeastern North Sea and Adjacent Onshore Areas*, J.P.H. Kaasschieter and T.J.A. Reijers (eds.), Geologie en Mijnbouw (1983) 157–168.

4. D'Heur, M.: "Chalk and Petroleum in North-West Europe," *Proc.*, 1989 Intl. Chalk Symposium, Brighton Polytechnic, 4–7 September. Thomas Telford, London (1990) 631.
5. Lind, I., Nykjær, O., Priisholm, S., and Springer, N.: "Permeability of Stylolite-Bearing Chalk," *JPT* (November 1994) 986.
6. Bowers, M.C., Ehrlich, R., and Clark R.A.: "Determination of Petrographic Factors Controlling Permeability Using Petrographic Image Analysis and Core Data, Satun Field, Pattani Basin, Gulf of Thailand," *Marine and Petroleum Geology* (1994) **11**, No. 2, 148.
7. Nelson, P.H.: "Permeability-Porosity Relationships in Sedimentary Rocks," *The Log Analyst* (May-June 1994) 38–62.
8. Carman, P.C.: "Fluid Flow Trough Granular Beds," *Trans*. Inst. Chem. Eng. London (1937)**15**, 150–166.
9. Wyllie, M.R.J. and Gardner, G.H.F.: "The Generalized Kozeny-Carman Equation. Its Application to Problems of Multiphase Flow in Porous Media," *World Oil* (March 1958) 121.
10. Beard, D.C. and Weyl, P.K.: "Influence of Texture on Porosity and Permeability of Unconsolidated Sand," *AAPG Bull*. (1973) **57**, No. 2, 349.
11. Nagtegaal, P.J.C.: "Sandstone-Framework Instability as a Function of Burial Diagenesis," *J. Geological Soc. London* (1978) **135**, 101.
12. Hartkamp, C.A., Arribas, J., and Tortosa, A.: "Grain Size, Composition, Porosity and Permeability Contrasts Within Cross-Bedded Sandstones in Tertiary Fluvial Deposits, Central Spain," *Sedimentology* (1993) **40**, 787.
13. Panda, M.N. and Lake, L.W.: "Estimation of Single-Phase Permeability From Parameters of Particle-Size Distribution," *AAPG Bull*. (1994) **78**, No. 7, 1028.
14. Niblack, W.: *An Introduction to Digital Image Processing*, Prentice-Hall, London (1986) 1–215.
15. Donaldson, E.C., Kendall, R.F., Baker, B.A., and Manning, F.S.: "Surface-Area Measurements of Geologic Materials," *SPEJ* (April 1975) 111.

Appendix

Kozeny's equation describes the flow through a porous homogeneous medium. It is written,

$$k = c \cdot \frac{\phi^3}{s^2}. \quad \text{(A-1)}$$

The factor c is an empirical constant, ϕ is the porosity, and S is the surface area per bulk volume.

Poiseuille's law for flow through parallel tubes in a solid medium can be written,

$$k = \tfrac{1}{2} \cdot r_h^2 \cdot \phi, \quad \text{(A-2)}$$

where the value ½ is the factor c in Kozeny's equation and r_h is the hydraulic radius, which is written as ϕ/S in Kozeny's equation.

Poiseuille's law is, thus, valid for flow in a porous medium with tubes in one direction. We wish to model flow through a reservoir rock by applying Poiseuille's law and must, therefore, quantify the proportion of the porosity that is open to flow in a given direction. This can be done by modeling a reservoir rock as a system of orthogonal interpenetrating tubes, allowing flow in three directions. **Fig. A-1** shows such a model in its simplest form. In Fig. A-1a, the porosity, ϕ, is shaded; in Fig. A-1b, only the porosity, ϕ_{af}, which is active for flow in a specific direction, is shaded.

To maintain the true porosity, ϕ, in the equation, we must correct the factor c for the ratio between porosity in the flow direction and the total porosity. The constant, c, valid for this model, will be

$$c = \frac{1}{2} \cdot \frac{\phi_{af}}{\phi} = \frac{\phi_{af}}{2 \cdot \phi}. \quad \text{(A-3)}$$

For porosities approaching zero, the factor c will approach ⅙, because the porosity will act as unconnected tubes so that $\phi_{af} = ⅓\phi$, while almost no porosity is shared by them. For unbounded porosity, c will approach ½, because, in each direction, all the porosity will be active in flow. We can express c as a function of porosity alone by the following calculations. If we look at a single tube-crossing in a cube of unit size, the porosity, ϕ, can be derived

a:

b:

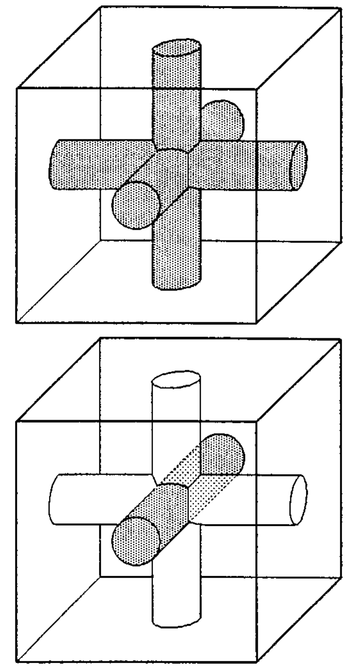

Fig. A-1—Porosity model. (a) All porosity is shown as shaded volume. (b) Here, only the porosity that is active for flow is shaded.

from the active flow porosity, ϕ_{af}, by

$$\phi = 3 \cdot \phi_{af} - V_1 - V_2, \quad \text{(A-4)}$$

where V_1 is the volume shared by two tubes, and V_2 is the volume representing the crossing of two tubes inside the third tube. The tube radius becomes $(\phi_{af}/\pi)^{1/2}$, so we obtain

$$\left.\begin{aligned} V_1 &= 16 \cdot \left(\frac{\phi_{af}}{\pi}\right)^{3/2} \int_{\omega_1} \sqrt{1 - x^2}\, dx\, dy \\ \omega_1 &= \{(x, y) | 0 \le x \le 1 \wedge 0 \le y \le x\} \end{aligned}\right\} \quad V_1 = \frac{16}{3}\left(\frac{\phi_{af}}{\pi}\right)^{3/2}$$

$$\left.\begin{aligned} V_2 &= 16 \cdot \left(\frac{\phi_{af}}{\pi}\right)^{3/2} \int_{\omega_2} \sqrt{1 - y^2}\, dx\, dy \\ \omega_2 &= \left\{(\theta, r) \middle| 0 \le \theta \le \frac{\pi}{4} \wedge 0 \le r \le 1\right\} \end{aligned}\right\} \Leftrightarrow$$

$$V_2 = 16 \cdot \left(\frac{\phi_{af}}{\pi}\right)^{3/2} \int_0^{\pi/4} \left(\int_0^1 \sqrt{1 - r^2 \sin^2\theta}\, r\, dr\right) d\theta$$

$$= 8 \cdot \left(\sqrt{2} - \frac{2}{3}\right) \cdot \left(\frac{\phi_{af}}{\pi}\right)^{3/2}$$

$$V_1 + V_2 = 8 \cdot \left(\frac{2}{3} + \sqrt{2} - \frac{2}{3}\right) \cdot \left(\frac{\phi_{af}}{\pi}\right)^{3/2}$$

$$= 8\sqrt{2} \cdot \left(\frac{\phi_{af}}{\pi}\right)^{3/2}. \quad \text{(A-5)}$$

By combining Eqs. A-4 and A-5 we obtain

$$\phi = 3 \cdot \phi_{af} - \frac{8 \cdot \sqrt{2}}{\pi^{3/2}} \cdot \phi_{af}^{3/2}. \quad \text{(A-6)}$$

Combination of Eqs. A-3 and A-6 results in the following algebraic equation.

$$k_1^3 - 12k_1^2 + 36k_1 - 8x^2\phi = 0, \quad \text{(A-7)}$$

where $k_1 = \frac{1}{c}$ and $x = \frac{8 \cdot \sqrt{2}}{\pi^{3/2}}$.

Solving Eq. A-7 for k_1 gives

$$k_1 = 4 \cos\left(\frac{1}{3}\arccos\left(\frac{\phi}{2}\frac{(\sqrt{2})^2 \cdot 8^2}{\pi^3} - 1\right) + \frac{4}{3}\pi\right) + 4,$$

$$c = \frac{1}{k},$$

and Kozeny's factor, c, thus becomes

$$c = \left(4 \cos\left(\frac{1}{3}\arccos\left(\phi\frac{8^2}{\pi^3} - 1\right) + \frac{4}{3}\pi\right) + 4\right)^{-1}. \quad \ldots\ldots (A\text{-}8)$$

If, instead of circular tubes, we make a similar model with square tubes, c will be

$$c = \left(4 \cos\left(\frac{1}{3}\arccos\left(\phi \cdot 2 - 1\right) + \frac{4}{3}\pi\right) + 4\right)^{-1}. \quad \ldots\ldots (A\text{-}9)$$

From Eqs. A-8 and A-9, c values can be calculated from the porosity as listed in Table 2. The values show that, whether the tubes have a circular or square cross section, the c factor for this model will be practically the same.

SI Metric Conversion Factors

ft × 3.04*	E−01	= m
md × 9.69 233	E−04	= μm^2
psi × 6.894 757	E+00	= kPa

*Conversion factor is exact.

Jeanette Mortensen is a petroleum engineer with Maersk Olie og Gas AS in Copenhagen. Previously, she worked on offshore drilling rigs in the North Sea and in the Arabian Gulf. She has also worked as a scientific officer at the Dept. of Geology and Geotechnical Engineering at Technical U. of Denmark. (DTU). Mortensen holds an MS degree in petroleum engineering from DTU. **Finn Engstrøm** is chief petrophysicst with Maersk Olie og Gas AS in Copenhagen. His research interests include general petrophysical models for chalk/carbonates, hydrodynamics/geodynamics, and fluid distribution modeling. He holds a PhD degree in electrophysics from DTU. Engstroem serves on the SPE Fluid Mechanics and Enhanced Oil Recovery Committee. **Ida Lind** is an associate professor at DTU, Dept. of Geology and Geotechnical Engineering, where her main responsibility is teaching and research in reservoir geology. She is engaged in studies of the diagenesis and reservoir properties of chalk. Previously, she worked for Maersk Oil and Gas AS. Lind holds a PhD degree in applied geology from DTU.


Mortensen


Engstrøm


Lind